JOURNAL OF MATERIALS SCIENCE 11 (1976) 333–340

Electrodiffusion damage in sodium chloride grain boundaries

L. B. HARRIS
School of Physics, University of New South Wales, P.O. Box 1, Kensington, N.S.W. 2033, Australia

The continuous passage of an electric current through pure sodium chloride bicrystals has been found to produce grain-boundary damage similar to that caused by electromigration in conducting thin films. The damage takes the form of an array of voids that seriously reduces the strength of the boundary. As in electromigration, the voids appear to be due to the condensation of vacancies following removal of ions by the current. However, the voids produced in tilt boundaries by current at 250° C have regularities of distribution and shape that suggest they are associated with separation of a second phase from segregated boundary impurity, the phase change disorder resulting from the precipitation reaction leading to rapid production of damage. The phase change process is discussed.

1. Introduction

The term electromigration is used to describe the flow of matter due to large direct electron or hole currents in conducting materials. In ionic solids, where a current represents the motion of ions, it is convenient to use the term electrodiffusion when referring to the transport of mass produced by the current. Low-temperature electromigration in thin conducting films produces damage in the form of irregular arrays of voids situated along grain boundaries [1], such damage being a serious cause of deterioration of the conducting elements in integrated circuit devices. It is reasonable to ask whether electrodiffusion can ever produce similar boundary damage in ionic solids, the much smaller currents in such poor conductors being compensated for by the much larger mass transport numbers. Order of magnitude calculation suggests that it can.

Electromigration current densities producing boundary damage are of the order of 10^6 A cm^{-2}, the corresponding mass transport numbers being of the order 10^{-7}. Current densities at sufficiently low temperatures for boundary transport to predominate over lattice transport in ionic solids would be not greater than 10^{-5} A cm^{-2}, the corresponding mass transport number being of order unity. Thus, the increase in transport number apparently fails by about 10^4 to compensate for the decrease in current. However, this naive calculation does not allow for the different mechanisms giving rise to mass transport in the two systems, nor for the different types of charge carrier. Since charge carriers in ionic solids are ions, values of enhanced grain-boundary diffusion that are 10^3 to 10^6 times diffusion within the lattice [2] imply that grain-boundary currents can similarly be 10^3 to 10^6 times lattice current and thus perhaps compensate locally for the shortfall factor of 10^4 mentioned above. There is no corresponding enhancement of the non-ionic boundary current in metals. Boundary damage in ionic solids would not be confined to thin films, since the heating effects of large currents that prevent low-temperature boundary damage in bulk metal samples are not operative during the electrodiffusion of bulk ionic solids.

It follows that any physical mechanism known to be associated with accelerated ion movement along boundaries stands a reasonable chance of also being associated with grain-boundary erosion. Such a mechanism is the preferential electrodecoration of grain boundaries at low temperatures [3, 4] which, for the particular case of electric fields of from 10^2 to 10^3 V cm^{-1} applied continuously to potassium bromide bicrystals at tempera-

tures of 200 to 250° C, was found to spread electrode silver over an entire grain-boundary plane in a remarkably short time. The speed at which such a distribution of silver was formed required values of boundary ion mobility to be many orders of magnitude larger than lattice mobility. It was considered [4] that the observed silver colloids could not have developed within the boundary unless there had been substantial electro-erosion of the boundary interface. Since decoration was often observed after only a few hours application of the field, compared with the weeks or months required to produce failure by boundary electromigration in conducting films, observation of the postulated boundary erosion should be relatively straightforward. The present work reports an attempt to produce and identify electrodiffusion damage in an alkali halide grain boundary under conditions similar to the previous electrodecoration experiments, but without the complicating presence of the silver colloids.

2. Experimental

The preparation of specimens, and the equipment used for observation, has been described previously [4]. In summary, bicrystal specimens some 3 or 4 mm thick and 20 mm in lateral dimension, containing a single plane grain boundary perpendicular to the large faces, were placed between electrodes in an oven with an observation window and subjected to fixed temperature and a continuous d.c. electric field, the boundary region being subsequently observed by optical microscope. In previous work with silver electrodes it was found that silver colloids were much less readily produced in NaCl than in KBr boundaries. This relative absence of colloids raised doubt as to whether boundary erosion had occurred in NaCl, though electrodiffusion behaviour in NaCl was not expected to be different from that in KBr. For this reason it was considered that NaCl was the more appropriate material for investigating the proposed boundary erosion in the absence of silver. Specimens were prepared containing 10° and 20° tilt boundaries, stainless steel electrodes being used to direct an electric field along the tilt axis. On the basis of earlier electrodecoration experiments, a field of 6×10^2 V cm^{-1} was used at a temperature of 250° C. The specimens were nominally pure, spectroscopic analysis showing that divalent cation impurity in the matrix (mainly calcium) was of the order of 1 ppm.

3. Observations

Electrodiffusion was found to produce a significant change in boundary strength. Prior to treatment the boundaries were mechanically strong, fracture at room temperature of the plate-like specimens occurring in single crystal alongside the central grain boundary. After electrodiffusion treatment, the specimens could be easily snapped at the boundary by hand. This was possible despite the fact that the volume of specimen lying within the projection of the electrodes, which were smaller than the specimen surface, included less than half of the total boundary plane. Some charge transport in the boundary outside the region projected from the electrodes would have been expected, however [3]. This drastic reduction in strength indicates a serious deterioration in bonding across the boundary due to the boundary current. Average current density through the specimen was of the order of 3×10^{-6} A cm^{-2}, but the proportion carried by the grain boundary is not known.

Microscope observation of fracture surfaces after treatment confirmed a deterioration in boundary structure. This deterioration was similar to that observed in electromigration damage, consisting of irregular arrays of voids. There was no indication of alkali metal colloids or dendrites, nor of colour centres, so the voids appear to be a direct physical consequence of the transport. On further examination it was found that both the morphology and the distribution of the voids contained certain regularities relating to the crystallography of the boundary and of the two adjoining half-crystals. The development of erosion in any particular boundary depended on the duration of the electrodiffusion, but after electrodiffusion lasting several days it was possible to distinguish uneven surface regions, relatively free of voids, that resembled conventional fractured surfaces, regions containing a regular distribution of voids of standard shape, and yet further regions containing irregular voids and indeterminate large-scale erosion. Heavy erosion that tended to form in the centre of the boundary where current flow was large was often accompanied by regular distributions of small voids near the periphery of the electrodes where current flow was smaller, so it is presumed that regular voids represent an earlier stage of erosion. On this basis the regions of uneven fracture without voids, which were scattered erratically across the boundary, could poss-

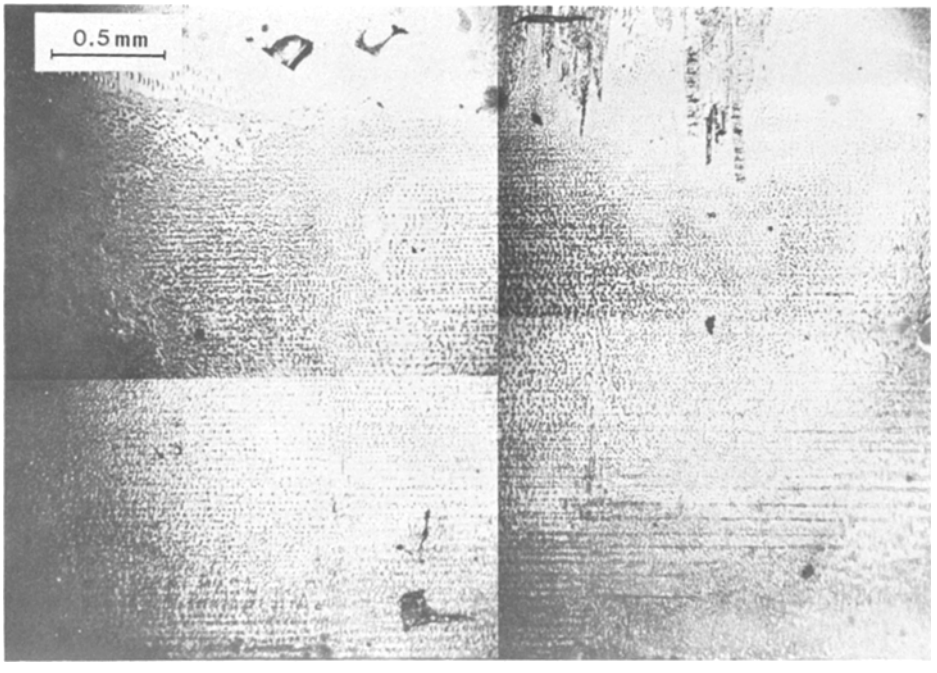

Figure 1 Grain-boundary fracture surface, 20° tilt boundary, compounded from separate exposures.

ibly be regions where current flow was very small due to some form of local inhomogeneity.

The common form of regular void structure is shown in Fig. 1, which is a micrograph of a fracture surface from a specimen in which electrodiffusion for 114 h had produced considerable erosion. The direction of the tilt axis is vertical, the field having been directed downwards towards the cathode surface of the specimen just visible at the bottom, while the growth direction of the bicrystal ingot from which the specimen was cut is horizontal. An array of pits is seen arranged in approximately parallel horizontal rows. At the top are fragments of conventional uneven fracture surface. In Fig. 2, which shows higher magnification views of two different areas in Fig. 1, the pits are seen to be some 5 to 10 μm in diameter. Not only are the pits to a large extent aligned along the growth direction, but there is also a general tendency for the pits to have a triangular shape, with the apex of all triangles pointing towards the left. There was some variation in triangular shape, however, the pits in Fig. 2a being rounded and approximately equilateral, while many of those in Fig. 2b are elongated vertically. In regions where erosion was heavier, these elongated pits tended to run together to form irregular vertical channels along the tilt axis. However, as seen in Fig. 2b, it was more usual for continuous channels to form along the growth direction.

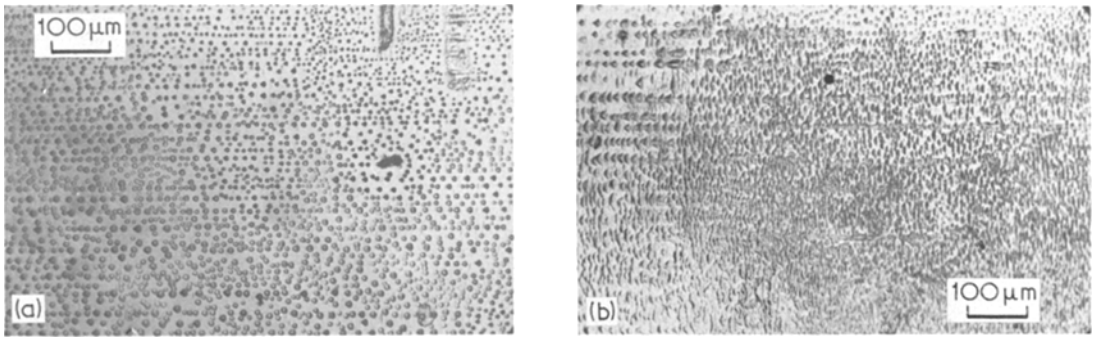

Figure 2 Enlarged view of different regions in Fig. 1 showing (a) triangular voids, (b) triangular and vertically elongated voids.

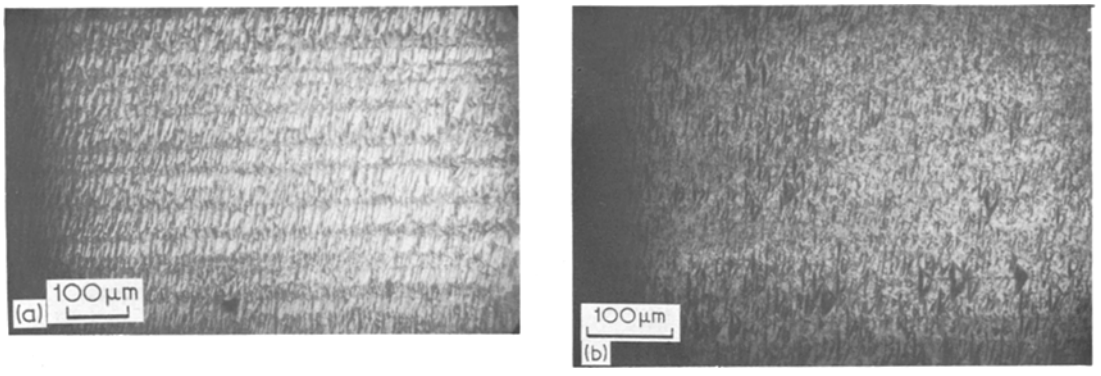

Figure 3 Etched grain-boundary fracture surface, 20° tilt boundary, showing (a) channels in growth direction, (b) systematically oriented triangular pits.

Fracture surfaces were etched in a saturated solution of mercuric chloride in ethyl alcohol, an etchant that produces square ⟨1 0 0⟩ dislocation etch pits. There was general attack over the whole surface, but the voids were not deepened, showing that dislocations were not the agents responsible for erosion. Fig. 3a shows a region of etched surface in which grooves in the growth direction are clearly seen, while Fig. 3b shows discrete triangular pits. Since Fig. 3 is a mirror image opposite half of the fracture surface seen in Fig. 2, the electric field having been applied vertically downwards in each case, the apex of each pit points to the right. Etching merely confirms the geometrical nature of the erosion defects.

The shape of the pits was examined in more detail, using a differential interference microscope to provide interference fringes and colour contrast across the pits. Pits from regions such as that shown in Fig. 2a had the shape shown in Fig. 4, the apex being found to point in the direction of convergence of the tilted (0 1 0) planes. The interior angle at A was less than 90° while that at B was much greater than 90°, the internal sides of the pit being steep near A but shallow near B. The shallow depression inside the region CBC of certain pits sometimes contained a small hump, and erosion appeared to be greatest in the chevron-shaped region CAC. There was a shallow depression, shown dotted in Fig. 4, surrounding the whole pit. Scanning of fracture surfaces revealed occasional triangular defects, such as those shown in Fig. 5, that appeared to be relatively unaffected by erosion. Presumably the defect seen in Fig. 5 gives rise to the pit shape shown in Fig. 4. Note that the base of the triangular defect in Fig. 5 lies along the [0 0 1] tilt-axis direction, but that the two sides adjacent to the apex intersect at an angle of 80° rather than the 90° required if these two sides were to coincide with ⟨1 0 1⟩ directions in the tilted (0 1 0) plane. The tilt of the (0 1 0) plane

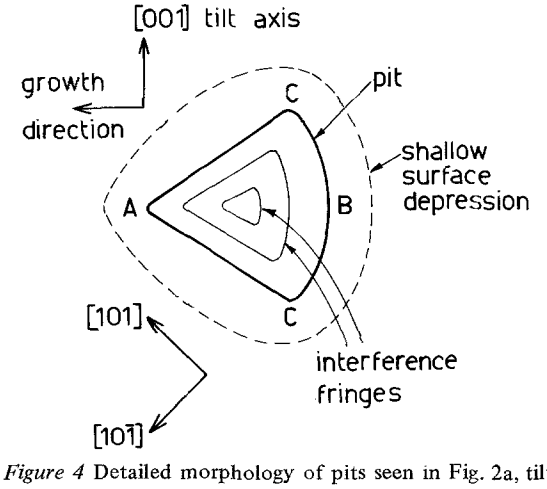

Figure 4 Detailed morphology of pits seen in Fig. 2a, tilt axis vertical, growth direction horizontal. Interference fringes reveal depth of pit; [1 0 1] and [1 0 $\bar{1}$] directions lie on (0 1 0) planes tilted at angle $\theta/2$ to observation plane.

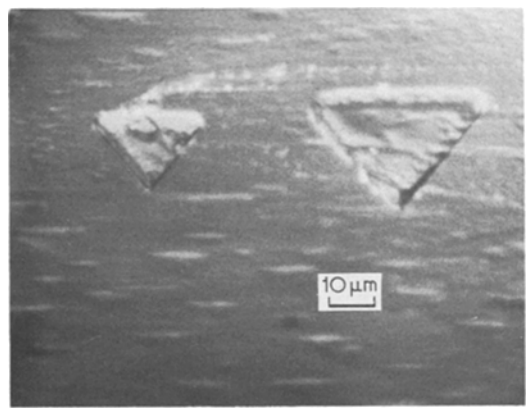

Figure 5 Triangular defects occasionally observed on fracture surface, tilt axis horizontal, growth direction vertical.

would make the apex angle appear slightly larger in the observation plane than it actually is.

Pit shapes in other regions of the fracture surface often had apex angles that were greater than 90° or an apex that was rounded into a smooth curve. Such pits are common in Fig. 2b, while the background region in Fig. 5 also shows a number of indistinct rounded-apex shapes. The basic void shape in the boundary plane is thus a triangle with its base along the tilt axis and an apex of varying angle that always points towards the convergence point of {0 1 0} planes. The pit contours at right angles to the boundary plane are not known in detail, though there was asymmetry in the growth direction, shown in Fig. 4 by biasing of the deepest point of the pit towards the apex. This asymmetry could be a consequence of boundary tilt, since the (0 1 0) lattice plane within which the pits are embedded lies at an angle $\theta/2$ to the observation plane, where θ is the tilt angle. From observation of interference fringes it was deduced that pit depth was 1 to 2 μm. The voids are thus seen to be triangular discs with slightly conical sides.

An additional corrosion feature of the fracture surface, noted when specimens were left exposed to the ambient atmosphere, was the formation of fine etch lines along the growth direction. Such an observation emphasizes the existence of a texture in the growth direction, which also gives rise to the horizontal channels seen in Figs. 2b and 3a.

4. Discussion

4.1. Electrodifusion damage and precipitation

Electromigration damage results from the accumulation of vacancies due to the sweeping away of ions by large electron flows [1]. Since current flow in the alkali halides is due to ion jumps between vacancy sites, it seems reasonable that electrodiffusion damage should also be due to the removal of ions by the current, although the rate of erosion appears to be far more rapid than could be provided by the normal rate of vacancy condensation at boundary sinks. The geometrical shape and regular distribution of the boundary voids suggests that erosion occurred at crystallographically definite sites within the boundary, and all evidence points to these being the sites of secondary phase particles that had separated out at the boundary. Although it was not possible to identify specific second phase particles, it is known from conductivity measurements that divalent cation impurity will precipitate out in the low temperature regions below about 200° C [5]. It has also been shown [2, 4] that segregation of impurity to the grain boundary, even in very pure crystals, can produce extremely high values of local impurity concentration in a narrow layer encompassing the boundary. By methods described elsewhere [4] it was established that boundary segregation had occurred in the bicrystals used in the present experiments, so it is assumed that precipitation at the boundary of impurities such as calcium and magnesium, especially the former, was highly probable.

The basis of the explanation of electrodecoration [4] was that the precipitation reaction in the boundary would produce local disorder and consequent enhanced charge transport over the precipitate–matrix interface, the rapid transport assigned to phase change disorder being similar to that which leads to high values of conductivity in superionic conductors [6]. Hence, the precipitate-matrix interface is the appropriate region for nucleation of the voids seen in the present work. It is not clear from the published literature whether the observed voids should be nucleated by the formation or by the dissolution of precipitate, particularly since the form the precipitation process takes in any particular specimen depends both on the thermal history of that specimen and on the concentration of impurity in it. Conductivity measurements [5] indicate that most precipitates rapidly dissolve in NaCl at 250° C, whereas light-scattering measurements [7, 8] suggest that the amount of precipitate in a NaCl sample is near to its maximum at this temperature. It is possible that conductivity and light scattering are, in fact, monitoring different stages of the precipitation reaction. Thus, the fact that precipitation of Ca in KCl is observed at grain boundaries by light scattering in the temperature range 275 to 350° C [9], and in single crystals by conductivity in the range 200 to 250° C [10, 11] may be due as much to the use of different experimental techniques as to differences in impurity concentration resulting from boundary segregation or other causes. Electrodecoration measurements on KBr [4] showed that grain-boundary fluidity at 300° C gave rise to a featureless form of erosion, in marked contrast with highly structured electrodecoration patterns obtained at 200° C. The fluidity at 300° C was assigned to dissolution of

boundary precipitates, in agreement with conductivity measurements on Ca-doped KBr single crystals [12] that show no precipitation at temperatures just above 300° C, while retention of boundary structure at 200° C was associated with a greatly reduced rate of dissolution. By analogy, electrodifussion damage in NaCl at 250° C could also be associated with slowly dissolving precipitate, the crystallographic orientation and regular distribution of voids in Figs. 2 to 5 indicating some retention of precipitate particle shape. The agreement is, as with KBr, with conductivity measurements [5]. It is shown below, however, that the formation of a precipitate particle is equally capable of leading to voids on the precipitate–matrix interface.

The most common metallic impurity was determined by spectroscopic analysis to be calcium, so it ought to be possible to relate the observed void shape to the structure of $CaCl_2$ particles that form in the NaCl lattice. The precursor stage of precipitation is the aggregation of divalent impurity-cation vacancy dipoles, and it has been suggested, quite generally, that the dipoles link together to form an hexagonal network in the {1 1 1} lattice planes [13]. However, a detailed study of the development of incipient precipitates of $CaCl_2$ in NaCl [14, 15] requires that platelets of $CaCl_2$ coherent with the matrix develop from {1 1 1} NaCl planes in which calcium-vacancy dipoles aggregate in rows, as in Fig. 6. Such a structure is more likely to develop from a lozenge trimer, of which a possible variant is shown in Fig. 6, than from an hexagonal one. Such a lozenge trimer is simply a three-dipole development of the linear dipole pair which Crawford [16] showed was favoured during the early stage of aggregation, and appears to be necessary to explain the preferential nucleation of precipitate [15] at $\frac{1}{2}\langle 1\,1\,0\rangle$ dislocations. The basically asymmetrical trimer, with its net dipole moment, can readily hook on to the dislocation line by means of a vacancy near the dislocation core, such as at point A in Fig. 6, for example. The build-up of this lozenge structure could give rise to a triangular shaped precipitate with edges along ⟨1 1 0⟩ directions, precipitate particles with edges lying close to this direction apparently being required for the triangular shape observed in Figs. 4 and 5. It is also to be noted that precipitation of $CaCl_2$ does not release the vacancies originally existing within the dipoles but incorporates them within the $CaCl_2$ structure, thus justifying the claim that precipitation removes cation vacancies from the matrix, leading to a reduction in conductivity.

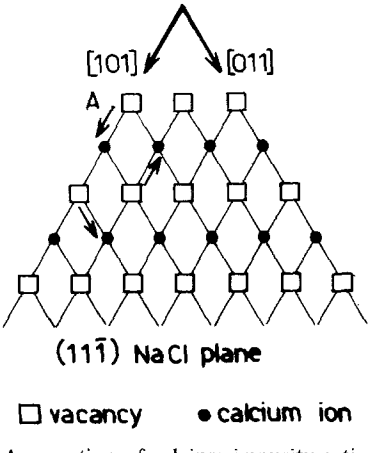

Figure 6 Aggregation of calcium impurity-cation vacancy pairs on a {1 1 1} sodium plane in NaCl, showing possible form of lozenge trimer. Trimer could nucleate on dislocation by vacancy at A.

The lattice separation between {1 1 1} planes in NaCl is slightly larger than the separation between the {1 0 0} planes of $CaCl_2$ into which they transform. Thus, as a precipitate particle develops it will grow out of register with and become detached from the matrix, and it has in fact been suggested [17] that a dense aggregate of precipitate platelets heated above 150° C transforms into a monolithic particle incoherent with the matrix. The interesting consequence is that the formation of precipitate, in the presence of electric current, could give rise to electrodiffusion damage observed as fissures at the precipitate–matrix interface due to transport in the incoherent region. Such electrodiffusion damage would proceed at a suitably rapid rate provided the phase transformation continued during current flow. Surface transport along structural mismatch regions in the absence of a phase transformation is part of the normal transport process and unlikely to give rise to local erosion except after much longer times of current flow.

4.2. Void shape and distribution

The observed disc-like voids co-planar with the boundary have the shape most likely to lead to a rapid decrease in boundary strength. This decrease becomes extreme when the voids begin to link up to form regions of open interface in which the two half-crystals are completely separate. Such separated regions have been observed in certain specimens.

There are four specific observations that allow void shape to be related to particular aspects of precipitation.

(1) The apex of each triangular void points towards the convergence of {0 1 0} planes, which means that impurity segregation and precipitation are directly influenced by boundary tilt.

(2) The void boundaries adjacent to the apex, observed on the boundary plane, often tend to lie close to ⟨1 1 0⟩ directions, which is compatible with {1 1 1} precipitate with a boundary along ⟨1 1 0⟩, as shown in Fig. 6.

(3) The voids observed in the boundary plane have a shallow depth. This is to be expected since impurity segregates in a narrow layer adjacent to the boundary, so that precipitate forms only within this layer. However, it means that a single precipitate platelet as a {1 1 1} plane will be restricted in growth away from the boundary.

(4) The base of the triangular voids (Figs. 4 and 5) lies along the tilt axis. Since the tilt axis is a structural axis that contains either dislocations or structural mismatches of dislocation type [18], it is to be expected that precipitates will preferentially nucleate along tilt axis structure.

On the basis of these four observations, it is possible to suggest that voids are formed by electro-erosion when a phase change reaction (probably dissolution) occurs, the electro-diffusion damage mirroring the distribution of precipitate in the boundary. The precipitate nucleates at tilt axis structure on a number of parallel {1 1 1} planes that intersect the boundary on {1 1 0} planes. The precipitate platelets do not extend laterally far from the boundary, but can spread within the boundary plane. It is equally possible to argue, however, that voids develop from precipitates in the form of the isotropic cylinders along ⟨1 1 0⟩ and ⟨1 0 0⟩ observed by light scattering [19]. Until the precise shape and distribution of the precipitate particles is known, as well as the variation of the precipitation reaction with temperature, it is not possible to be more specific.

Some variation in void shape is to be expected from the fact that, when impurity is segregated to a grain boundary, the grain-boundary region is a layer of finite thickness and not an infinitely thin plane [2]. Hence, precipitate will tend to nucleate, not on a single plane but at points spread over the thickness of this layer, so that the voids will have a similar lateral spread. The result is that a fracture plane, such as that seen in Fig. 2 will not pass through the centre of all voids, so that a variation in void shape, such as the observed spread in apex angle, is to be expected.

The existence of precipitate aggregates some 5 μm in linear extent in nominally pure bicrystals is not surprising, since enhanced grain-boundary diffusion allows the impurity ions to collect together into a precipitate particle much more rapidly than in single crystals. Precipitation centres in doped single crystals have been observed to have a separation of the order 10 μm [20], which is comparable to void separation in the boundary in Fig. 2, in which segregation apparently produced comparable values of local doping. Further, the void size is comparable with the size (5 μm^2) of the regions of optical inhomogeneity observed in as-grown NaCl twist bicrystals [21], the preferred explanation for these regions being that they are boundary second phase [2].

The regularity seen in Figs. 2 and 3, and in particular the existence of definite lines of voids along the growth direction calls for some comment, since it is not the form to be expected from a purely random aggregation process. In parts of certain boundaries there appears to be a more or less regular sub-lattice of precipitation sites, though there are other regions where void distribution is entirely irregular. If, as suggested in observation 4 above, precipitate nucleates at tilt-axis structure (vertical in Fig. 3), then either such structure does not persist over macroscopic distances or precipitate nucleates as discrete particles in a random fashion on this structure. By contrast, a regular form of growth structure (horizontal) is often markedly evident. This growth structure, which appears to be related to how impurities are incorporated during solidification, suggests a regular but inhomogeneous distribution of impurities in the boundary. Like the orientation of triangular voids along the growth direction, it must for the present remain unexplained. It is noted that electrodecoration of NaCl bicrystals [22], which produces a cross-grid structure in which silver colloids are aligned in the growth direction, the silver colloids presumably occupying electro-erosion voids, is further evidence of precipitation lining up along the growth direction.

The observation of grain-boundary damage by electrodiffusion in ionic solids is not surprising, in view of previous report of rapid damage produced by a phase change. This latter observation suggests a possible mechanism for the rapid migration of

certain metallic ions in some oxides under the influence of an electric field, which leads to a deterioration in insulating properties. Once electro-erosion associated with precipitation has occurred, the ions may find it easy to migrate over the surfaces so formed. This may be part explanation of the migration of the chromium ion in alumina [23].

Acknowledgement

Most of the microphotography in this work was carried out by Mr P. G. Quang.

References

1. F. M. D'HEURLE and R. ROSENBERG, *Phys. Thin Films* **7** (1973) 257.
2. W. D. KINGERY, *J. Amer. Ceram. Soc.* **57** (1974) 1, 74.
3. L. B. HARRIS and J. L. SCHLEDERER, *Acta Met.* **19** (1971) 577.
4. L. B. HARRIS, *Phil. Mag.* to be published.
5. R. W. DREYFUS and A. S. NOWICK, *Phys. Rev.* **126** (1962) 1367.
6. W. J. PARDEE and G. D. MAHAN, *J. Solid State Chem.* to be published.
7. I. BALTOG, C. GHITA and M. GUIRGEA, *J. Phys. C: Solid State Phys* **7** (1974) 1892.
8. M. I. ABAEV and M. I. KORNFELD, *Soviet Phys. – Solid State* **7** (1966) 2271.
9. G. HAURET and M. GIRARD-NOTTIN, *Phys. Stat. Sol.* **17** (1966) 881.
10. G. KUMBARTZKI and K. THOMMEN, *Z. Phys.* **184** (1965) 355.
11. F. FROHLICH and G. HENSEL, *Phys. Stat. Sol.* **24** (1967) 535.
12. S. CHANDRA and J. ROLFE, *Canad. J. Phys.* **49** (1971) 2098.
13. J. S. COOK and J. S. DRYDEN, *Proc. Phys. Soc.* **80** (1962) 479.
14. K. SUZUKI, *J. Phys. Soc. Japan* **10** (1955) 794.
15. K. YAKI and G. HONJO, *ibid* **22** (1967) 610.
16. J. H. CRAWFORD, *J. Phys. Chem. Solids* **31** (1970) 399.
17. K. SUZUKI, *J. Phys. Soc. Japan* **13** (1958) 179.
18. G. H. BISHOP and B. CHALMERS, *Scripta Met.* **2** (1968) 133.
19. M. NOTTIN, *Acta Cryst.* **A26** (1970) 636.
20. K. G. BANSIGIR and E. E. SCHNEIDER, *J. Appl. Phys. Suppl.* **33** (1962) 383.
21. M. L. GIMPL, A. D. MCMASTER and N. FUSCHILLO, "Ceramic Microstructures", edited by R. M. Fulrath and J. A. Pask (John Wiley, New York, 1968) p.253.
22. L. B. HARRIS, *J. Crystal Growth* **24/25** (1974) 410.
23. A. J. MOULSON, W. R. PHILLIPS and P. POPPER, "Special Ceramics 1964", edited by P. Popper (Academic Press, London, 1965) p. 199.

Received 30 May and accepted 21 July 1975.